Electronic transport properties of an (8, 0) carbon/boron nitride nanotube heterojunction*

Liu Hong-Xia(刘红霞)[a)†], Zhang He-Ming(张鹤鸣)[a)],
Song Jiu-Xu(宋久旭)[a)], and Zhang Zhi-Yong(张志勇)[b)]

[a)] *Key Laboratory of Ministry of Education for Wide Band-Gap Semiconductor Materials and Devices, School of Microelectronics, Xidian University, Xi'an* 710071, *China*

[b)] *Information Science and Technology Institution, Northwest University, Xi'an* 710069, *China*

(Received 15 March 2009; revised manuscript received 30 September 2009)

The structure of a heterojunction made up of an (8, 0) carbon nanotube and an (8, 0) boron nitride nanotube is achieved through geometry optimization implemented in the CASTEP package. Based on the optimized geometry, the model of the heterojunction is established. Its transport properties are investigated by combining the nonequilibrium Green's function with density functional theory. Results show that both the lowest unoccupied molecular orbital and the highest occupied molecular orbital mainly locate on the carbon nanotube section. In the current–voltage characteristic of the heterojunction, a rectification feature is revealed.

Keywords: nanotube heterojunction, nonequilibrium Green's function, transport properties

PACC: 7115M, 7125X, 6600

1. Introduction

Since the discovery of carbon nanotubes (CNTs),[1] they have attracted a lot of attention because of their unique properties and potential applications in nanoelectronics. In recent years, many other nanotubes have been synthesized, such as SiGe nanotubes,[2] BN nanotubes,[3−5] and GaN nanotubes,[6] which provide the foundation of fabrication for heterojunctions made up of different nanotubes. A heterojunction made up of CNT and CNx nanotube was realized by using the chosen synthesis method, and a rectifying property was discovered.[7] The transport properties of the nanotube heterojunction are rarely studied, thereby restricting their modeling and applications.

The method where the nonequilibrium Green's function (NEGF) is combined with density functional theory (DFT) is widely used in studies of the transport properties of the molecular devices and some characteristics have been discovered in these devices.[8−11] Some studies on nanotube electronic devices have been performed with this method. Li *et al* studied the influence of nanotube size on the transport properties of nanotube heterojunctions.[12] The working mechanism of nanotube Schottky diodes was achieved and a rectifying characteristic was found in their current–voltage curves.[13] Some field-effect transistors have been prepared with nanotube arrays. The effect of coupling between adjacent nanotubes in the arrays on their transport properties was also found.[14]

In the present paper, the structure of a heterojunction made up of an (8, 0) CNT and an (8, 0) BNNT is achieved through geometry optimization implemented in the CASTEP package. Based on the above structure, a two-probe model is established. With the method combining NEGF with DFT, the transport properties of the heterojunction are investigated. We find that there is a transmission gap in the transmission spectrum of the heterojunction. The lowest unoccupied molecular orbital and the highest occupied molecular orbital have higher electron density on the CNT section. Rectifying behaviour is also revealed. Our results are helpful to the fabrication and applications of heterojunctions.

2. Model and method

The transport properties of the heterojunction are determined by its structure to some degree. Before the study on the transport properties of the heterojunction, the geometry optimization was implemented.

*Project supported by the Chinese Defence Advance Research Program of Science and Technology, China (Grant No. 9140A08060407DZ0103).

†Corresponding author. E-mail: liuhongxia_xidian@126.com

© 2010 Chinese Physical Society and IOP Publishing Ltd

Through geometry optimization on the heterojunction, the structure that is closest to the actual configuration can be achieved. Therefore, a supercell was established (shown in Fig. 1), in which 64 C atoms, 32 N atoms and 32 B atoms were included. The supercell was large enough for calculation.[15] Geometry optimization on the heterojunction was realized with the CASTEP package based on DFT.[16,17] In calculations, the exchange–correlation functional was described by the generalized gradient approximation (GGA). The electronic wave functions were expanded by the plane wave basis set and ultrasoft pseudopotentials were used to describe the electron–ion interaction. Brillouin zone integrations were realized with the Monkhorst–Pack method and a 1×1×8 k-point sampling was used. The geometry was not stopped until convergence conditions were satisfied, where the force, the stress and the displacement of each atom are set to be less than 0.05 eV/Å, 0.05 GPa and 5×10^{-4} Å (1 Å=0.1 nm) respectively.

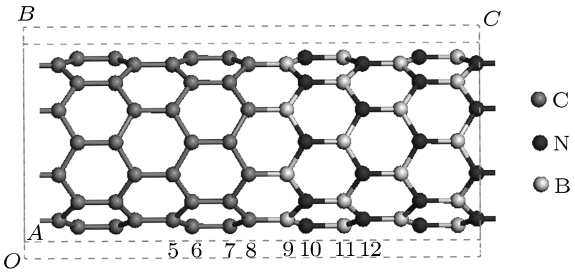


Fig. 1. A supercell of an (8, 0) carbon/boron nitride nanotube heterojunction.

The variations of the structure can be achieved by comparing the radii of C layers, B layers and N layers in the heterojunction with those of the isolated nanotubes. The structures of the isolated CNT and BNNT were also optimized with the CASTEP package. The diameter of the (8, 0) CNT is 6.264 Å and is consistent with the result of Song *et al.*[18] The B–N bond length in BNNT is 1.44 Å and agrees with Zhang *et al.*'s calculations.[19] The diameters of the nitrogen layers and the boron layers are 6.449 Å and 6.356 Å, respectively. The diameters of the C layers, B layers and N layers near the interface of the heterojunction are shown in Table 1. It can be seen that the maximal changes of the diameter lie in layer 8 and layer 9. With the increase of the distance from the interface of the heterojunction, the changes of the diameters decrease sharply. The variations of the fourth layer in the CNT and BNNT section are −0.004 Å(about 0.0639%) and −0.007 Å(about 0.109%), which can be ignored. From the above analysis, we can see that the size of the supercell is large enough to include the variation of the heterojunction in geometry.

Table 1. Diameters of layers in the heterojunction and their changes.

layer type	layer number	diameter/Å	ΔD/Å
C	5	6.260	–0.004
C	6	6.273	0.009
C	7	7.280	0.016
C	8	6.348	0.084
B	9	6.324	–0.032
N	10	6.456	0.007
B	11	6.375	0.019
N	12	6.442	–0.007

To investigate the transport properties of the heterojunction, a two-probe system was built based on the above optimized structure (in Fig. 2), which is larger than the above supercell. The two-probe system can be divided into three parts: left semi-infinite electrode, central scattering region, and right semi-infinite electrode. The structures of the left and right semi-infinite electrodes were the same as the individual CNT and BNNT. The central scattering region was composed of the CNT section and BNNT section. There were 13 C layers in the CNT section, while in the BNNT section 8 B layers and 7 N layers could be found. Periodic boundary conductions were imposed on the surface parallel to the flat formed by a certain C layer, N layer or B layer.

The transport properties of the above system were explored with the fully self-consistent NEGF method implemented in the TranSIESTA-C package and its latest version, Atomistix ToolKit 2.3 (ATK 2.3). This method has been successfully applied to the study on the transport properties of molecular devices. In our calculations, the GGA was adopted to describe the exchange–correlation energy. The valence electrons were expanded in a numerical atomic-orbital basis set of single zeta (SZ). Core electrons were modeled with Troullier–Martins local pseudopotentials.[20]

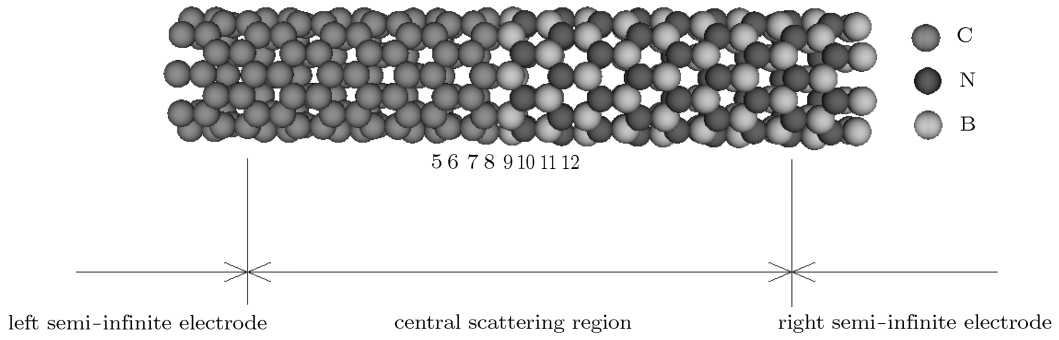


Fig. 2. Schematic illustration of a two-probe system for a CNT/BNNT heterojunction.

The transmission spectrum means the probability for an electron with incident energy E under bias voltage V to transfer from the left semi-infinite electrode to the right and is calculated by

$$T(E,V) = \mathrm{tr}[\boldsymbol{\Gamma}_{\mathrm{L}}(E,V)G(E,V)\boldsymbol{\Gamma}_{\mathrm{R}}(E,V)G^{\dagger}(E,V)], \tag{1}$$

where $G(E,V)$ is the Green's function of the two-probe system, and $\boldsymbol{\Gamma}_{\mathrm{L/R}}$ is the coupling matrix. The integration of the transmission spectrum yields the current through the system

$$I(V) = \int_{\mu_{\mathrm{L}}}^{\mu_{\mathrm{R}}} T(E,V)[f(E-\mu_{\mathrm{L}}) - f(E-\mu_{\mathrm{R}})]\mathrm{d}E, \tag{2}$$

where $\mu_{\mathrm{L}} = -V/2(\mu_{\mathrm{R}} = +V/2)$ is the chemical potential of the left (right) electrode.

3. Results and discussion

With no bias voltage applied, the equilibrium transport properties of the above two-probe system were studied firstly. The transmission coefficients of the heterojunction as a function of electron energy are shown in Fig. 3. A transmission gap (transmission coefficient is zero) about 2.8 eV is observed to be near zero. In the negative energy region, there are three steps starting at −0.52 eV, −1.84 eV and −2.54 eV, separately.

The molecular projected self-consistent Hamiltonian (MPSH) can be achieved through projecting the self-consistent Hamiltonian onto the Hilbert space spanned by the basis functions of the central atoms. The eigenstates of MPSH are related to the poles of the Green's function and roughly correspond to the peaks in the transmission spectrum.[8] To understand the steps in Fig. 3, we calculated the frontier molecular orbitals of the MPSH for the heterojunction.

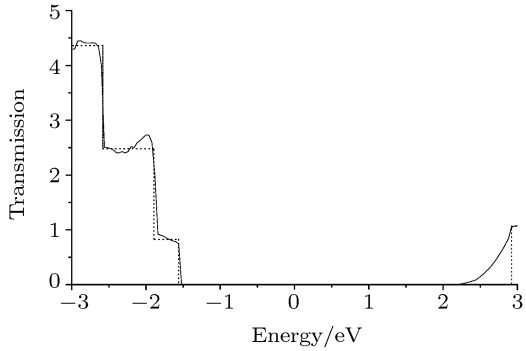


Fig. 3. Transmission coefficient of the heterojunction.

Six frontier molecular orbitals of the MPSH for the heterojunction are shown in Fig. 4. The lowest unoccupied molecular orbital (LUMO, O_2) and the highest occupied molecular orbital (HOMO, O_3) each have a higher electron density on the CNT section. The eigenenergies of these two orbitals are +1.08 eV and −0.69 eV, which means that the energy gap of the heterojunction is about 1.77 eV. As the localities of the above orbitals are high, no transmission steps are formed at the corresponding energies. The increase of the transmission coefficient starting at +2.83 eV is the result of the orbital O_1 with an eigenvalue of +2.78 eV. The three transmission steps in the negative energy range come from the other three orbitals O_4, O_5 and O_6, which have eigenvalues of −1.60 eV, −2.38 eV and −2.90 eV, respectively.

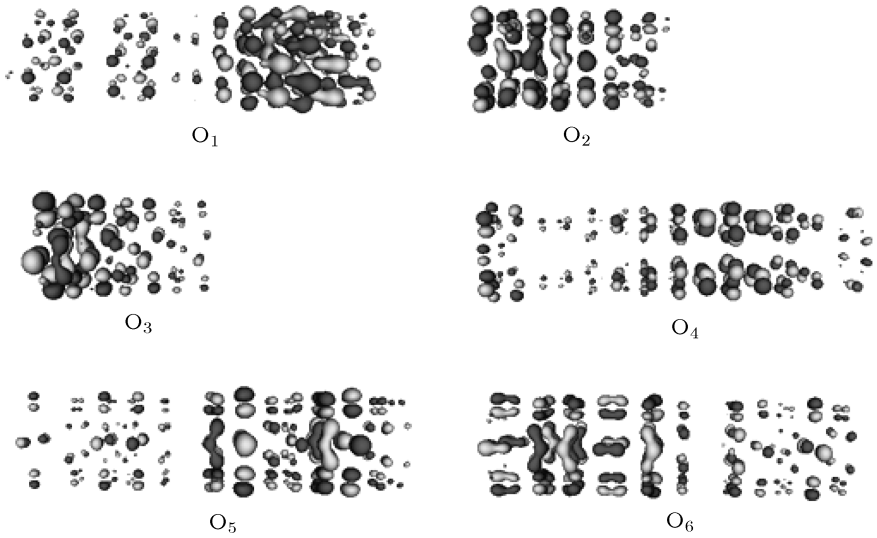


Fig. 4. Frontier orbitals of MPSH for the heterojunction, CNT section in the left part of the orbital and BNNT section in the right part.

Figure 5 describes the current as a function of applied bias voltage for the heterojunction. Under each bias, the electronic structure is determined self-consistently under the nonequilibrium conditions. The current is calculated by the Landauer–Büttiker formula:

$$I(V) = \int_{\mu_{\rm L}}^{\mu_{\rm R}} T(E,V)[f(E-\mu_{\rm L}) - f(E-\mu_{\rm R})]{\rm d}E,$$

where $T(E,V)$ is the transmission probability for electrons at incident energy E through the heterojunction under a bias V.

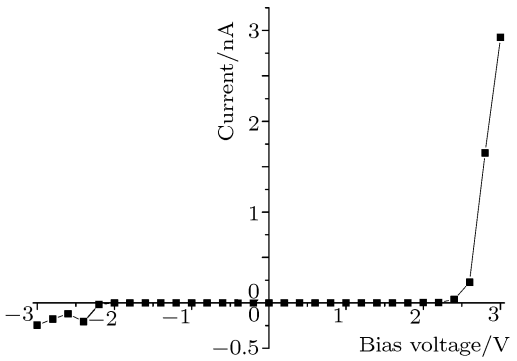


Fig. 5. I–V curve of heterojunction.

The current–voltage curve for the heterojunction was obtained through the above calculations (in Fig. 5). As the calculation is time-consuming work, the bias was taken to range from −3.0 V to +3.0 V. Self-consistent calculations were performed for each bias value. We can see from the figure that for the positive bias, before the bias reaches +2.4 V the heterojunction has a zero current. When the bias equals and exceeds +2.4 V, the current increases steeply. For the negative bias, the current is nearly zero before −2.2 V. From −2.2 V to −2.4 V, the current has a trivial increase. However, there is a small dip in the I–V curve between −2.4V and −2.6 V. Then the current increases slowly again with the increase of the bias. But the magnitude of the current under the negative bias is much smaller than that of the positive current. We believe that the negative current is saturated.

From Eq. (2), we can see that the current flowing through the heterojunction is determined by transmission spectrum and the energy range (bias window), in which the integral is realized. Owing to the fact that the biases applied to the electrodes are $\pm V/2$, the bias windows under +3.0 V and −3.0 V are [−1.5, 1.5]. As the bias windows have the same sizes, the current is determined by the transmission spectrum. To ascertain the difference between the current of the heterojunction under negative bias and under positive bias, the transmission spectra in the bias window under +3.0 V and −3.0 V were calculated.

There is a transmission peak at +1.28 eV in the transmission spectrum of the heterojunction under the bias of −3.0V (Fig. 6(a)). This transmission peak plays an important role in forming the current under this bias. The current of the heterojunction under +3.0 V is determined by the transmission peak at

−0.66 eV to some degree (Fig. 6(b)). The width and the peak value of the later transmission peak are much greater than those of the former, which results in the difference between the current under +3.0 V and under −3.0 V. Through the above analysis, we roughly understand the origin of the current variations under positive and negative biases, while the I–V curve must be further studied, which is the basis of its application.

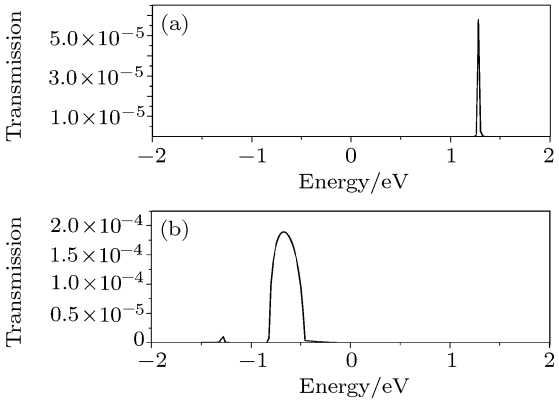


Fig. 6. Transmission spectra of the two-probe system for the heterojunction under bias −3.0 V (a) and +3.0V (b).

4. Conclusions

To investigate the transport properties of the heterojunction made up of CNT and BNNT, the structure of the heterojunction is obtained through geometry optimization implemented in the CASTEP package. A two-probe system is built based on the optimized structure of the heterojunction, whose transport properties are studied by the method combing NEGF with DFT. The LUMO and HOMO of the heterojunction each have a higher electron density on the CNT section. The current increases more quickly under positive bias than under negative bias and the current under negative bias tends to be saturated. Our results are helpful for modeling nanotube heterojunction devices.

Acknowledgement

We thank Atomistix for their trial version of Atomistix ToolKit 2.3 (ATK 2.3).

References

[1] Iijima S 1991 *Nature* **354** 56
[2] Huczko A, Bystrzejewski M, Lange H, Fabianowska A, Cudzilo S, Panas A and Szala M 2005 *J. Phys. Chem.* B **109** 16244
[3] Lourie O R, Jones C R, Bartlett B M, Gibbons P C, Ruoff R S and Buhro W E 2000 *Chem. Mater.* **12** 1808
[4] Ciuparu D, Klie R F, Zhu Y M and Pfefferle L 2004 *J. Phys. Chem.* B **108** 3967
[5] Bechelany M, Bernard S, Brioude A, Cornu D, Stadelmann P, Charcosset C, Fiaty K and Miele P 2007 *J. Phys. Chem.* C **111** 13378
[6] Moradian R, Azadi S and Farahani S V 2008 *Phys. Lett.* A **372** 6935
[7] Chai Y, Zhou X L, Li P J, Zhang W J, Zhang Q F and Wu J L 2005 *Nanotechnology* **16** 2134
[8] Li Z Y and Kosov D S 2006 *J. Phys. Chem.* B **110** 9893
[9] Chen J Z, Zhang J and Han R S 2008 *Chin. Phys.* B **17** 2208
[10] Niu X M and Qi H Y 2008 *Acta Phys. Sin.* **57** 6926 (in Chinese)
[11] Long M Q, Chen K Q, Wang L L and Zou B S 2007 *Appl. Phys. Lett.* **91** 233512
[12] Li X F, Chen K Q, Wang L L, Long M Q and Zou B S 2007 *Appl. Phys. Lett.* **91** 133511
[13] Bai P, Li E, Lam K T, Kurniawan O and Koh W S 2008 *Nanotechnology* **19** 115203
[14] Tzolov M, Chang B, Yin A, Straus D, Xu J M and Brown G 2004 *Phys. Rev. Lett.* **92** 075505
[15] Thesing L A, Piquini P and Kar T 2006 *Nanotechnology* **17** 1637
[16] Wei J W, Hu H F, Zeng H, Zhou Z P, Yang W W and Peng P 2008 *Phys.* E **40** 462
[17] Pan H, Feng Y P and Lin J Y 2006 *Phys. Rev.* B **73** 035420
[18] Song C, Xia Y Y, Zhao M W, Liu X D, Li F and Huang B D 2005 *Chem. Phys. Lett.* **415** 183
[19] Zhang J, Loh K P, Yang S W and Wu P 2005 *Appl. Phys. Lett.* **87** 243
[20] Wang Z C, Kadohira T, Tada T and Watanabe S 2007 *Nano. Lett.* **7** 2688